

Neutrino mass bounds from DESI 2024 are relaxed by Planck PR4 and cosmological supernovae

Itamar J. Allali^a Alessio Notari^{b,c}

^aDepartment of Physics, Brown University, Providence, RI 02912, USA

^bDepartament de Física Quàntica i Astrofísica & Institut de Ciències del Cosmos (ICCUB), Universitat de Barcelona, Martí i Franquès 1, 08028 Barcelona, Spain.

^cGalileo Galilei Institute for theoretical physics, Centro Nazionale INFN di Studi Avanzati Largo Enrico Fermi 2, I-50125, Firenze, Italy

E-mail: itamar_allali@brown.edu, notari@fqa.ub.edu

Abstract. The recent DESI 2024 Baryon Acoustic Oscillations (BAO) measurements combined with the CMB data from the Planck 18 PR3 dataset and the Planck PR4+ACT DR6 lensing data, with a prior on the sum of the neutrino masses $\sum m_\nu > 0$, leads to a strong constraint, $\sum m_\nu < 0.072$ eV, which would exclude the inverted neutrino hierarchy and put some tension on even the standard hierarchy. We show that actually this bound gets significantly relaxed when combining the new DESI measurements with the HiLLiPoP + LoLLiPoP likelihoods, based on the Planck 2020 PR4 dataset, and with supernovae datasets. We note that the fact that neutrino masses are pushed towards zero, and even towards negative values, is known to be correlated with the so-called A_L tension, a mismatch between lensing and power spectrum measurements in the Planck PR3 data, which is reduced by HiLLiPoP + LoLLiPoP to less than 1σ . We find $\sum m_\nu < 0.1$ eV and $\sum m_\nu < 0.12$ eV, with the supernovae *Pantheon+* and *DES-SN5YR* datasets respectively. The shift caused by these datasets is more compatible with the expectations from neutrino oscillation experiments, and both the normal and inverted hierarchy scenarios remain now viable, even with the $\sum m_\nu > 0$ prior. Finally, we analyze neutrino mass bounds in an extension of Λ CDM that addresses the H_0 tension, with extra fluid Dark Radiation, finding that in such models bounds are further relaxed and the posterior probability for $\sum m_\nu$ begins to exhibit a peak at positive values.

Contents

1	Introduction	1
2	Models and datasets	2
3	New constraints on neutrino masses in ΛCDM+$\sum m_\nu$	3
3.1	Effects of Planck Likelihoods	4
3.2	Effects of Supernovae likelihoods	5
3.3	Effects of BAO measurements	6
3.4	Estimates of Bayesian Evidence for Mass Ordering	6
4	Constraints on neutrino masses in extensions with Dark Radiation	7
5	Conclusions	8
A	Combined analysis with SH0ES	12
B	Neutrino mass posteriors fit to a Gaussian	13
C	Constraints from various BAO measurements	14

1 Introduction

Cosmological observations are at present the most promising way to detect for the first time the sum of neutrino masses. Nonetheless, the recent combination of datasets presented by the Dark Energy Spectroscopic Instrument (DESI) collaboration [1], including their new data release on Baryon Acoustic Oscillations (BAO) together with the Planck CMB 2018 data [2] (the `Planck`, `Commander`, and `SimAll` likelihoods based on the 2018 PR3 dataset on Temperature and Polarization, together with the `NPIPE` PR4 Planck CMB lensing reconstruction [3] and the lensing data from the Data Release 6 of the Atacama Cosmology Telescope [4]), is showing only a (quite stringent) upper bound on the sum of neutrino masses, $\sum m_\nu < 0.072$ eV [1], when imposing the most conservative prior $\sum m_\nu > 0$. There is no hint of a nonzero mass and the posterior probability actually shows a cusp at zero, so that the peak of the distribution, if extended with a Gaussian [5], would even go to (unphysical) negative values (see also [6]). Since positive neutrino masses imply a suppression of the matter power spectrum, this would mean that such data prefer an enhancement of the spectrum.

However, it is known that this preference in the direction of negative values is correlated to the lensing “anomaly,” or tension, present in the likelihoods based on Planck 2018 data [2], i.e the fact that the ad hoc parameter A_L , that rescales the deflection power spectrum used to lens the primordial CMB power spectra, is larger than 1 when it is left free to vary, instead of being consistent with its real value $A_L = 1$. Forcing $A_L = 1$ pushes instead the neutrino masses towards negative values [2]. Recently, new likelihoods for the final (PR4) Planck CMB data release have been published [7], both for high- ℓ TT, TE and EE spectra (`HiLLiPoP`) and

for the low- ℓ EE polarization spectra (LoLLiPoP), to be used together with the Planck18 low- ℓ TT data. Such new likelihoods have been shown to lead to $A_L = 1.039 \pm 0.052$ in Λ CDM, consistent with the expected value of unity. It has been already shown using CMB data alone [7], that as a result of this shift, the neutrino masses move to more positive values.

The aim of this work is to assess the status of the preference for positive neutrino masses employing such new CMB likelihoods, combined together with the new released BAO data from galaxies and quasars [8] at redshifts $0.3 \lesssim z \lesssim 1.5$ and from the Lyman- α forest [9] by DESI [1] 2024. We will also check the impact on neutrino masses of Supernovae datasets, i.e. Pantheon+ [10] and DES-SN5YR [11].

We will analyse such bounds in the context of the Λ CDM model, with varying neutrino masses. Subsequently, we will also consider neutrino mass bounds in extensions of the Λ CDM model that have been recently proposed to address the Hubble tension with the addition of a Dark Radiation (DR) component [12].

In all the analyses, we will apply a prior $\sum m_\nu > 0$, i.e. we assume here no prior information from neutrino oscillation experiments, in order to have a fully independent measurement of neutrino masses.

2 Models and datasets

We will first study the simple Λ CDM spatially-flat cosmological model with free sum of neutrino masses, the Λ CDM+ $\sum m_\nu$ model. We assume for simplicity the three neutrinos to have the same mass, since it has been shown that current experiments are sensitive only to the sum of neutrino masses, irrespective of how are they distributed [13].

We perform a Bayesian analysis using CLASS [14, 15] to solve for the cosmological evolution and either MontePython [16, 17] or Cobaya [18, 19] to collect Markov Chain Monte Carlo (MCMC) samples. We obtain posteriors and figures using GetDist [20]. We consider various combinations of datasets, as follows.

In Section 3.1 we will explore three different Planck likelihoods for CMB data:

- **P18**: the Planck 2018 high- ℓ TT, TE, EE Plik, low- ℓ TT Commander, and low- ℓ EE SimAll likelihoods, together with the Planck 2018 lensing data [21];
- **P20_H**: the HiLLiPoP + LoLLiPoP likelihoods [7], based on the final Planck data release (PR4) [22]. In particular: the HiLLiPoP likelihood at high- ℓ for TT, TE, EE; the LoLLiPoP likelihood for low- ℓ EE; the Planck 2018 Commander likelihood for low- ℓ TT and Planck 2018 CMB lensing data [21];
- **P20_C**: The CamSpec likelihood [23], updated by [24] to the 2020 Planck PR4 data release [22], at high- ℓ for TT, TE, EE; the Planck 2018 Commander and SimAll likelihoods for low- ℓ TT and EE, respectively, and the Planck 2020 PR4 lensing likelihood [3].

Then, in Section 3.2, we will explore the effects of including different sets of cosmological supernovae:

- **Pantheon**: The Pantheon+ supernovae compilation [10].
- **DES-SN**: The DES-SN5YR supernovae compilation [11].

For most of this work, we will focus on the BAO measurements from DESI. In Section 3.3, we will also compare to other BAO measurements. The BAO datasets under consideration are:

- **DESI**: BAO measurements from DESI 2024 [1] at effective redshifts $z = 0.3, 0.51, 0.71, 0.93, 1.32, 1.49, 2.33$;
- **SDSS₁₆**: BAO measurements from 6dFGS at $z = 0.106$ [25]; SDSS MGS at $z = 0.15$ [26]; and SDSS eBOSS DR16 measurements [5], including DR12 galaxies [27], and DR16 LRG [28, 29], QSO [30, 31], ELG [32, 33], Lyman- α , and Lyman- $\alpha \times$ QSO [34].
- **SDSS_{f σ_8}** : The same BAO measurements given in **SDSS₁₆**, while using the full-shape likelihoods for LRG, ELG, QSO, Lyman- α , and Lyman- $\alpha \times$ QSO [5], which include constraints on $f\sigma_8$ from redshift-space distortions.
- **DESI/SDSS**: BAO measurements from the combination suggested in [1] that merges DESI 2024 with previous SDSS measurements, choosing for each bin the measurement with the highest precision to date.

After discussing the status of neutrino masses in the simplest setup, we will also extend our analysis to models beyond Λ CDM, that have recently been shown to address the so-called Hubble tension, i.e. the tension on the determination of the present Hubble rate from the above datasets with the following local direct measurement of the expansion rate by the SH0ES collaboration:

- **H₀**: the measurement of the intrinsic SNIa magnitude $M_b = -19.253 \pm 0.027$ [35], which uses a Cepheid-calibrated distance ladder. We add this always in combination with Pantheon+ data, as implemented in the `Pantheon_Plus_SH0ES` likelihood in `MontePython`.¹

Such models extend Λ CDM by including a new Dark Radiation (DR) component, which lowers the tension [12], below 3σ and as low as 1.8σ , depending on the specific realization (free-streaming or fluid DR, present before BBN or produced after BBN²) and on the combination of datasets. Given the lower degree of tension, we are allowed in this case to combine with the **H₀** measurement, interpreting the tension as a moderate statistical fluctuation. In Section 4, we will focus on one particular choice for the DR, the fluid DR present before the epoch of BBN, for simplicity.

3 New constraints on neutrino masses in Λ CDM + $\sum m_\nu$

In this section we conservatively consider the Λ CDM model with variable neutrino masses, even if such model is: (1) in strong tension with SH0ES, and (2) mildly disfavoured compared to time varying dark-energy scenarios when not considering SH0ES (e.g. with respect to the so-called w_0w_a CDM model [1], which however points to the unphysical region with equation of state $w < -1$, or physically viable models, such as the “ramp” quintessence model [37]).

¹An even newer measurement from the collaboration is given in [36], but we use the value in [35] because of the available combination with Pantheon+.

²We note that constraints from primordial element abundances, which we do not include in this work, are not relevant when DR is produced after BBN.

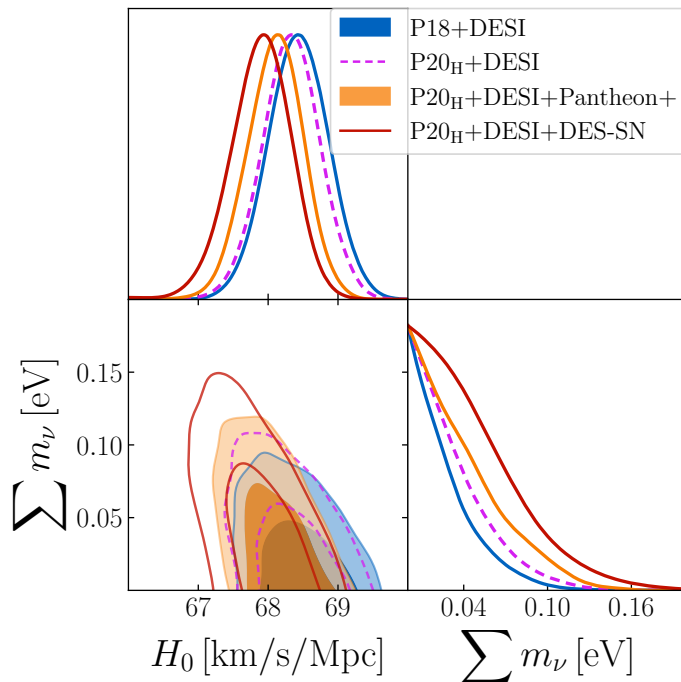


Figure 1: One- and two-dimensional posteriors for H_0 and $\sum m_\nu$ in the Λ CDM + $\sum m_\nu$ model, fitting to combinations of the Planck 2018 likelihoods with DESI BAO, compared to using the Planck 2020 HiLLiPoP + LoLLiPoP likelihoods with DESI BAO and the sets of cosmological supernovae from Pantheon+ and DES-SN5YR.

Within the Λ CDM + $\sum m_\nu$ model, the DESI collaboration finds [1] $\sum m_\nu < 0.072$ eV (95%CL, using DESI and Planck 2018 TT, TE, EE likelihoods, with PR4+ACT DR6 lensing data), which improves substantially on the analogous previous bound, $\sum m_\nu < 0.12$ eV (95%CL, from Planck 2018 combined with SDSS DR12 BAO [2]). At face value, this new bound excludes the inverted hierarchy case ($\sum m_\nu > 0.10$ eV) and starts to put some pressure even on the normal hierarchy case³. The situation, however, changes substantially when exploring various combinations of datasets, as discussed below.

3.1 Effects of Planck Likelihoods

First, we discuss the effect of including more recent Planck likelihoods, from the PR4 2020 data release. The bound gets substantially relaxed by making use of the recent HiLLiPoP + LoLLiPoP (**P20_H**) likelihoods, leading to:

$$\sum m_\nu < 0.086 \text{ eV (95\%CL, P20}_H\text{+DESI)}.$$

The weakening of the bound compared to the case with **P18** is consistent with the expectation that a smaller A_L should lead to larger neutrino masses [7, 21, 38]. Note that we compare here to our **P18** combination which uses the Planck 2018 lensing, giving $\sum m_\nu < 0.073$ eV (see Table 1), rather than comparing to the constraint in [1] which uses a different lensing likelihood.

³Note however that such a strong conclusion is not robust under the change of prior, i.e. it does not hold when using the prior based on neutrino oscillations, $\sum m_\nu > 0.06$ eV.

Dataset	$\sum m_\nu$	Dataset	$\sum m_\nu$
P18+DESI	< 0.073	P20_C+DESI	< 0.080
+ Pantheon	< 0.086	P20_H+SDSS₁₆	< 0.14
+ DES-SN	< 0.094	P20_H+SDSS_{fσ_8}	< 0.11
P20_H+DESI	< 0.086	P20_H+DESI/SDSS	< 0.11
+ Pantheon	< 0.099	+ Pantheon	< 0.12
+ DES-SN	< 0.11	+ DES-SN	< 0.13

Table 1: 95%CL upper bounds on the neutrino mass sum for Λ CDM + $\sum m_\nu$ model, comparing fits to various datasets.

Using instead the **CamSpec** likelihood which has also been updated to PR4, we find an intermediate result:

$$\sum m_\nu < 0.080 \text{ eV (95\%CL, P20}_C\text{+DESI)}.$$

These constraints, as well the constraint from the combination of data **P18** defined above, are summarized in Table 1. In addition, in Fig. 1, one can compare the posteriors of $\sum m_\nu$ for **P18+DESI** and **P20_H+DESI**, noting that the latter contour shows a relaxed constraint.

Since **P20_H** and **P20_C** use the most up-to-date set of data from Planck, and further, since it has been shown that **HiLLiPoP+LoLLiPoP** have been the most effective at eliminating the A_L problem in the Planck data, we will take the combination **P20_H** to be the preferred Planck dataset for the remainder of this work.

3.2 Effects of Supernovae likelihoods

Adding supernovae, the bounds get further relaxed

$$\sum m_\nu < 0.099 \text{ eV (95\%CL, P20}_H\text{+DESI+Pantheon)},$$

$$\sum m_\nu < 0.11 \text{ eV (95\%CL, P20}_H\text{+DESI+DES-SN)}.$$

The fact that **DES-SN** leads to higher neutrino masses compared to **Pantheon** is consistent with the earlier analysis in [2]. Table 1 gives a summary of these constraints, including the combination of **P18** with supernovae data; we note that the addition of supernovae to **P18** has a similar shift to the replacement of **P18** by **P20_H** (note also that this shift by adding Pantheon+ has been noticed in [39]).

The resulting probability distributions are presented in Fig. 1. As one can see, the preferred neutrino masses move to more positive values compared to the **P18+DESI** case (see Appendix B), which looks promising in view of more precise measurements, from DESI or Euclid [40], that could finally confirm a detection of neutrino masses from cosmological data in the region allowed by oscillation experiments $\sum m_\nu > 0.06$. The inverted hierarchy scenario is also currently still allowed by the **P20_H+DESI+DES-SN** combinations (and only marginally disfavored when considering **P20_H+DESI+Pantheon**), even with the $\sum m_\nu > 0$ prior.

We note that with supernovae data, the addition of more data provides a weaker bound, rather than a stronger one. This is an indication that the datasets in combination here are mildly in tension with respect to the effects of nonzero neutrino mass.

3.3 Effects of BAO measurements

We also investigate here the effect of using other BAO datasets, instead of DESI. Using the most recent eBOSS DR16 measurements from SDSS [5] (in combination with 6DFGS [25] and older data from SDSS) the bound is substantially weaker:

$$\sum m_\nu < 0.14 \text{ eV (95\%CL, P20}_H\text{+SDSS}_{16}) .$$

The eBOSS BAO measurements can be also combined with $f\sigma_8$ measurements from redshift-space distortions [5], which has more constraining power:

$$\sum m_\nu < 0.11 \text{ eV (95\%CL, P20}_H\text{+SDSS}_{f\sigma_8}) .$$

Finally, we used the combination of SDSS and DESI as described in [1], leading to

$$\sum m_\nu < 0.11 \text{ eV (95\%CL, P20}_H\text{+DESI/SDSS}) .$$

This can be considered the state-of-the-art combination, since it uses the measurement with the best BAO statistical power in each redshift bin; this status will shift as DESI releases more data in the future. Note, however, that this combines data processed with different methods/pipelines, and the combination has not been fully validated. We can see here that, with this combination, both inverted and normal hierarchy for the neutrino mass are allowed at 95% confidence level.

3.4 Estimates of Bayesian Evidence for Mass Ordering

One of the goals of this work has been to evaluate whether the BAO measurements from DESI constitute strong evidence against the inverted mass ordering. To that end, we can compute the Bayes factor (BF), the ratio of the models' evidences in two models, via the Savage-Dickey ratio. For a model M_1 nested within an encompassing model M_0 , the ratio is given by the ratio of the marginal posterior of M_0 evaluated in the limit where it is equivalent to M_1 divided by the prior of M_0 in the same limit. To evaluate the evidence for or against the inverted mass ordering, let us consider the encompassing model M_0 to be the one with the sum of the neutrino masses unconstrained $\sum m_\nu > 0$ and the nested model M_1 to have a nonzero lower bound $\sum m_\nu > m_1$. Then, the Bayes factor computed via the Savage-Dickey ratio is written explicitly as

$$BF_{10} \equiv \frac{P(\mathcal{D}|M_1)}{P(\mathcal{D}|M_0)} = \frac{P(\sum m_\nu > m_1|\mathcal{D}, M_0)}{P(\sum m_\nu > m_1|M_0)} \quad (3.1)$$

where BF_{10} is the Bayes factor of comparing M_1 to M_0 ; $P(\mathcal{D}|M_j)$ is the model evidence, i.e. the probability of the data \mathcal{D} given the model M_j ; $P(\sum m_\nu > m_1|\mathcal{D}, M_0)$ is the marginalized posterior of the parameter $\sum m_\nu$ integrated over the domain $\sum m_\nu \in [m_1, \infty)$, or the probability of obtaining $\sum m_\nu > m_1$ given \mathcal{D} and M_0 ; and $P(\sum m_\nu > m_1|M_0)$ is the prior on $\sum m_\nu$ for model M_0 , integrated over the domain $\sum m_\nu \in [m_1, \infty)$. Since we do not bound the domain for the prior on $\sum m_\nu$, we can approximate $P(\sum m_\nu > m_1|M_0) \approx 1$ in the limit where the prior is very broad.⁴

⁴This approximation introduces an error roughly proportional to the fraction of prior volume contained in the nested model; if the prior boundary was $[0, m_2]$, then the estimated BF would be altered by a factor of $1 - m_1/m_2$. Since we evaluate evidence based on $\ln BF$, this error is only $|\ln(1 - m_1/m_2)| \approx m_1/m_2 \ll 1$ for $m_1 \ll m_2$.

Dataset	$\ln BF_i$	$\ln BF_{i/n}$
P18+DESI	-4.5	-2.2
P20_H+DESI	-3.7	-1.8
P20_H+DESI+DES-SN	-2.4	-1.2

Table 2: The natural logarithm of the Bayes factors providing evidence for inverted hierarchy $\ln BF_i$ and evidence for inverted over normal hierarchy $\ln BF_{i/n}$, computed via the Savage-Dickey ratio, for several datasets.

Then, if we wish estimate the evidence for or against the inverted mass ordering, we can do this approximately by computing the Bayes factor for a model with a lower bound $m_1 = 0.1$ eV, which we will denote BF_i . Note, however, that since this domain also includes normal hierarchy, the Bayes factor may be overestimated (though we do not expect a large change in $\ln BF_i$). The natural logarithms of these Bayes factors are given in Table 2. Based on, e.g. [41], we can consider $|\ln BF| < 1.0$ to be inconclusive, $1 < |\ln BF| < 2.5$ to be “weak” evidence, $2.5 < |\ln BF| < 5.0$ to be “moderate” evidence, and $|\ln BF| > 5.0$ to be “strong” evidence. Therefore, we can see that while the combination of **P18+DESI** provides moderate to strong evidence against the inverted mass ordering, the evidence becomes more moderate with the replacement of **P18** with **P20_H**, dropping even to the “weak” evidence category when combined with **DES-SN**.

If instead of evaluating the direct evidence for or against inverted mass ordering, one wishes to compare the evidence of one ordering over the other, we could compute the same ratio as in Eq. (3.1), replacing the encompassing model with the model corresponding to normal ordering $\sum m_\nu > 0.06$ eV. This is equivalent to the ratio of the individual Bayes factors for each model (normal and inverted) with respect to the encompassing model M_0 ($\sum m_\nu > 0$). In this approach, we find the Bayes factor for inverted ordering with respect to normal ordering $BF_{i/n}$ and report them in Table 2. In each case, we find the preference for normal ordering over inverted to be only weak, with the combination **P18+DESI+DES-SN** nearing on inconclusive.

4 Constraints on neutrino masses in extensions with Dark Radiation

Let us first point out the fact that, in Λ CDM, the sum of the neutrino masses is negatively correlated with H_0 , as seen in Fig. 1. Thus, one may anticipate that a combined analysis with SHOES would drive the fit towards smaller (or even negative, see [5, 6]) neutrino masses. This is precisely the case in Λ CDM, where it is actually inconsistent to combine with SHOES (+**H₀**; see Appendix A for further discussion of this effect).

On the other hand, in the Dark Radiation (DR) models which alleviate the Hubble tension [12], one may suspect that the same negative correlation exists. However, nonzero neutrino mass exhibits a slight positive correlation with the DR abundance ΔN_{eff} , defined as the effective number of extra neutrino species $\Delta N_{\text{eff}} \equiv \rho_{\text{DR}}/\rho_\nu$, with ρ_{DR} and ρ_ν being the energy densities of DR and one neutrino species, respectively. Since it is known that H_0 and ΔN_{eff} are positively correlated, the end result for the correlation of $\sum m_\nu$ and H_0 is not obvious.

We highlight the case of a perfect (self-interacting) fluid DR, over the case where DR is free-streaming, given that the fluid DR relaxes the Hubble tension more significantly [12]. We show results in Table 3 and in Fig. 2 for the fluid DR model across several datasets. We

Dataset	$\sum m_\nu$
P20_H+DESI+Pantheon	< 0.13
P20_H+DESI+Pantheon+H₀	< 0.15
P20_H+DESI+DES-SN	< 0.15
P20_H+DESI/SDSS+Pantheon	< 0.15
P20_H+DESI/SDSS+DES-SN	< 0.17

Table 3: 95%CL upper bounds on the neutrino mass sum for the Λ CDM + Fluid DR + $\sum m_\nu$ model, comparing different datasets.

focus on the case where the fluid is present during the epoch of big-bang nucleosynthesis (BBN), but we have checked that the conclusions regarding neutrino mass are unaltered for the case where DR is produced after BBN.

Looking first at the constraints on the neutrino mass in Table 3, we find overall larger values for the sum of neutrino masses within DR models compared to the Λ CDM model. Computing Bayes Factors as in the previous section, we find that the evidence against inverted hierarchy is consistently weak in the datasets presented in Table 3, as low as $\ln BF_i \approx -1.2$ for **P20_H+DESI/SDSS+DES-SN**. Comparing, instead, with respect to normal ordering, the evidence is inconclusive ($|\ln BF_{i/n}| \lesssim 1$).

Next, it can be appreciated in Fig. 2 that the degeneracy between H_0 and $\sum m_\nu$ exhibited in Λ CDM has been broken, and there is no longer a correlation. It is not surprising, therefore, that we see that the addition of the **H₀** dataset does not substantially alter the neutrino mass bound in Table 3 (see Appendix A for further comparison). Moreover, we can see in Fig. 2 that the posteriors for $\sum m_\nu$ are beginning to form peaks at nonzero values (see Appendix B for a discussion of the peak locations). For example, with the dataset **P20_H+DESI/SDSS+DES-SN**, we see a clear peak in the posterior at a value $\sum m_\nu \sim 0.04$ eV, which is $< 0.5\sigma$ away from the expected value of 0.06 eV from neutrino oscillation experiments. Therefore, in the context of the fluid DR model as a solution to the Hubble tension, it is conceivable that a small increase in precision from upcoming data may also lead to the detection of neutrino masses. Note that all of the cases presented in Fig. 2 exhibit a $< 3\sigma$ tension with SH0ES; however, the case with the highest neutrino masses also exhibits the highest degree of tension with SH0ES, so it remains important to understand this interplay further.

5 Conclusions

The new DESI 2024 data release, combined with Planck18 CMB data, at face value leads to a strong bound on neutrino masses in the Λ CDM model [1], when assuming a $\sum m_\nu > 0$ prior, which excludes the inverted hierarchy scenario and seems to go even in the direction of negative masses [5, 6]. We have shown that these conclusions do *not* hold when using more recent Planck 2020 likelihoods (HiLLiPoP+LoLLiPoP), in combination with cosmological supernovae, since both go in the direction of favoring more positive masses. Concretely, we showed that the Bayesian evidence (quantified by Bayes factors) trends from moderate to weak evidence against inverted hierarchy when including these data, as well as from weak towards inconclusive evidence for normal ordering over inverted. This can be emphasized by extending the posteriors for $\sum m_\nu$ to negative values by fitting to a Gaussian; Fig. 3 shows that the peaks of the would-be posteriors are shifted towards positive values by adding

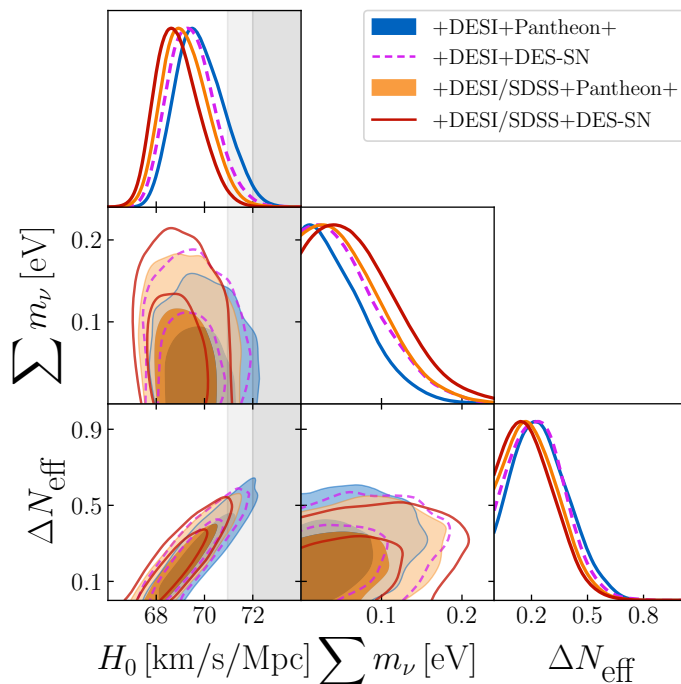


Figure 2: One- and two-dimensional posteriors for H_0 , $\sum m_\nu$, and ΔN_{eff} in the fluid DR model, fitting to combinations of **P20H** with either **DESI** or **DESI/SDSS**, and either **Pantheon** or **DES-SN**. The inner and outer two-dimensional contours give the 1- and 2- σ confidence intervals, respectively. The dark and light gray bands show the 1- and 2- σ confidence intervals from the measurement of H_0 by the SH0ES collaboration.

more data, especially in the case of DES supernovae (see Appendix B for more details). The distributions are peaked at even larger positive values of $\sum m_\nu$ for the fluid DR model, closer to the expected lower bound of $\sum m_\nu > 0.06$ eV from neutrino oscillations. We find the conservative upper bound at 95%CL to be $m_\nu < 0.12$ eV ($m_\nu < 0.1$ eV) when adding also DES-SN5YR (or Pantheon+) supernovae.

Furthermore, we have analyzed neutrino mass bounds in a model with fluid Dark Radiation that addresses the Hubble tension [12], and we have shown that in this case: (i) neutrino mass bounds are driven to even larger values, (ii) bounds are robust when combining with the SH0ES measurement of H_0 , and (iii) posterior probabilities even peak at nonzero neutrino masses.

Even if our findings go in the direction of relaxing constraints, they in fact constitute a significant improvement in the consistency with the expectation of $\sum m_\nu \geq 0.06$ eV that comes from neutrino oscillation experiments. Overall, our results represent a promising starting point in the quest for neutrino mass detection with upcoming cosmological data.

Acknowledgments

We thank Fabrizio Rompineve and Marko Simonovic for useful discussions. The work of A.N. is supported by the grants PID2019-108122GB-C32 from the Spanish Ministry of Science and Innovation, Unit of Excellence Maria de Maeztu 2020-2023 of ICCUB (CEX2019-000918-M) and AGAUR 2021 SGR 00872. The work of I.J.A. is supported by NASA grant

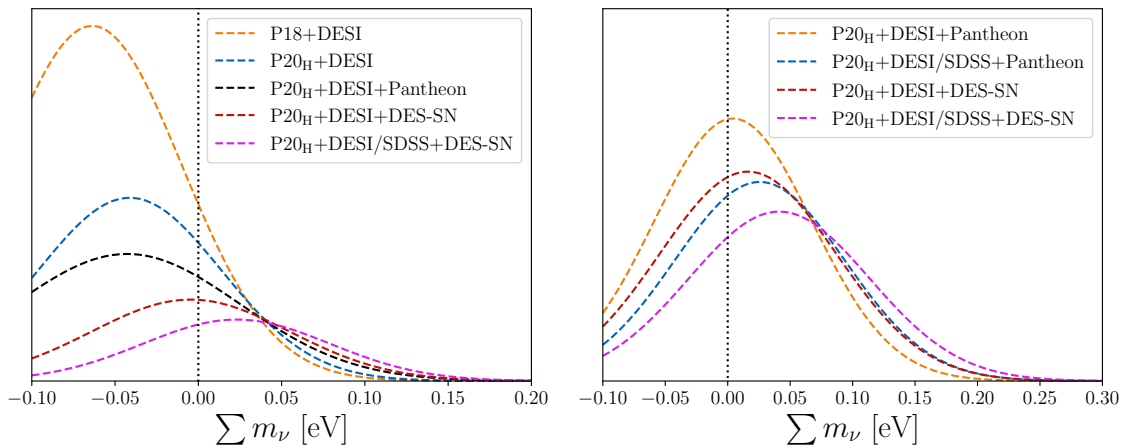


Figure 3: Posterior distributions for $\sum m_\nu$, inferred with the prior $\sum m_\nu > 0$, are fit to Gaussian distributions and extended for $\sum m_\nu < 0$ to project the approximate location of the peak preferred by the data. These curves are normalized such that the portion with $\sum m_\nu > 0$, corresponding to the posteriors from the MCMC analysis, integrates to unity. The left side figure shows various fits for the $\Lambda\text{CDM} + \sum m_\nu$ model, while the right side shows the $\Lambda\text{CDM} + \sum m_\nu + \text{Fluid DR}$ model.

80NSSC22K081. A.N. is grateful to the Physics Department of the University of Florence for the hospitality during the course of this work. Part of this work was conducted using computational resources and services at the Center for Computation and Visualization, Brown University. We also acknowledge use of the INFN Florence cluster.

References

- [1] DESI collaboration, *DESI 2024 VI: Cosmological Constraints from the Measurements of Baryon Acoustic Oscillations*, [2404.03002](#).
- [2] PLANCK collaboration, *Planck 2018 results. VI. Cosmological parameters*, *Astron. Astrophys.* **641** (2020) A6 [[1807.06209](#)].
- [3] J. Carron, M. Mirmelstein and A. Lewis, *CMB lensing from Planck PR4 maps*, *JCAP* **09** (2022) 039 [[2206.07773](#)].
- [4] ACT collaboration, *The Atacama Cosmology Telescope: A Measurement of the DR6 CMB Lensing Power Spectrum and Its Implications for Structure Growth*, *Astrophys. J.* **962** (2024) 112 [[2304.05202](#)].
- [5] EBOSS collaboration, *Completed SDSS-IV extended Baryon Oscillation Spectroscopic Survey: Cosmological implications from two decades of spectroscopic surveys at the Apache Point Observatory*, *Phys. Rev. D* **103** (2021) 083533 [[2007.08991](#)].
- [6] N. Craig, D. Green, J. Meyers and S. Rajendran, *No ν_s is Good News*, [2405.00836](#).
- [7] M. Tristram et al., *Cosmological parameters derived from the final Planck data release (PR4)*, *Astron. Astrophys.* **682** (2024) A37 [[2309.10034](#)].
- [8] DESI collaboration, *DESI 2024 III: Baryon Acoustic Oscillations from Galaxies and Quasars*, [2404.03000](#).
- [9] DESI collaboration, *DESI 2024 IV: Baryon Acoustic Oscillations from the Lyman Alpha Forest*, [2404.03001](#).

- [10] D. Scolnic et al., *The Pantheon+ Analysis: The Full Data Set and Light-curve Release*, *Astrophys. J.* **938** (2022) 113 [2112.03863].
- [11] DES collaboration, *The Dark Energy Survey: Cosmology Results With ~ 1500 New High-redshift Type Ia Supernovae Using The Full 5-year Dataset*, **2401.02929**.
- [12] I.J. Allali, A. Notari and F. Rompineve, *Dark Radiation with Baryon Acoustic Oscillations from DESI 2024 and the H_0 tension*, **2404.15220**.
- [13] CORE collaboration, *Exploring cosmic origins with CORE: Cosmological parameters*, *JCAP* **04** (2018) 017 [1612.00021].
- [14] J. Lesgourgues, *The Cosmic Linear Anisotropy Solving System (CLASS) I: Overview*, **1104.2932**.
- [15] D. Blas, J. Lesgourgues and T. Tram, *The Cosmic Linear Anisotropy Solving System (CLASS) II: Approximation schemes*, *JCAP* **07** (2011) 034 [1104.2933].
- [16] B. Audren, J. Lesgourgues, K. Benabed and S. Prunet, *Conservative Constraints on Early Cosmology: an illustration of the Monte Python cosmological parameter inference code*, *JCAP* **02** (2013) 001 [1210.7183].
- [17] T. Brinckmann and J. Lesgourgues, *MontePython 3: boosted MCMC sampler and other features*, *Phys. Dark Univ.* **24** (2019) 100260 [1804.07261].
- [18] J. Torrado and A. Lewis, *Cobaya: Code for Bayesian Analysis of hierarchical physical models*, *JCAP* **05** (2021) 057 [2005.05290].
- [19] J. Torrado and A. Lewis, “Cobaya: Bayesian analysis in cosmology.” Astrophysics Source Code Library, record ascl:1910.019, Oct., 2019.
- [20] A. Lewis, *GetDist: a Python package for analysing Monte Carlo samples*, **1910.13970**.
- [21] PLANCK collaboration, *Planck 2018 results. V. CMB power spectra and likelihoods*, *Astron. Astrophys.* **641** (2020) A5 [1907.12875].
- [22] PLANCK collaboration, *Planck intermediate results. LVII. Joint Planck LFI and HFI data processing*, *Astron. Astrophys.* **643** (2020) A42 [2007.04997].
- [23] G. Efstathiou and S. Gratton, *A Detailed Description of the CamSpec Likelihood Pipeline and a Reanalysis of the Planck High Frequency Maps*, **1910.00483**.
- [24] E. Rosenberg, S. Gratton and G. Efstathiou, *CMB power spectra and cosmological parameters from Planck PR4 with CamSpec*, *Mon. Not. Roy. Astron. Soc.* **517** (2022) 4620 [2205.10869].
- [25] F. Beutler, C. Blake, M. Colless, D.H. Jones, L. Staveley-Smith, L. Campbell et al., *The 6dF Galaxy Survey: Baryon Acoustic Oscillations and the Local Hubble Constant*, *Mon. Not. Roy. Astron. Soc.* **416** (2011) 3017 [1106.3366].
- [26] A.J. Ross, L. Samushia, C. Howlett, W.J. Percival, A. Burden and M. Manera, *The clustering of the SDSS DR7 main Galaxy sample – I. A 4 per cent distance measure at $z = 0.15$* , *Mon. Not. Roy. Astron. Soc.* **449** (2015) 835 [1409.3242].
- [27] BOSS collaboration, *The clustering of galaxies in the completed SDSS-III Baryon Oscillation Spectroscopic Survey: cosmological analysis of the DR12 galaxy sample*, *Mon. Not. Roy. Astron. Soc.* **470** (2017) 2617 [1607.03155].
- [28] EBOSS collaboration, *The Completed SDSS-IV extended Baryon Oscillation Spectroscopic Survey: measurement of the BAO and growth rate of structure of the luminous red galaxy sample from the anisotropic correlation function between redshifts 0.6 and 1*, *Mon. Not. Roy. Astron. Soc.* **500** (2020) 736 [2007.08993].
- [29] EBOSS collaboration, *The Completed SDSS-IV extended Baryon Oscillation Spectroscopic Survey: measurement of the BAO and growth rate of structure of the luminous red galaxy*

- sample from the anisotropic power spectrum between redshifts 0.6 and 1.0, *Mon. Not. Roy. Astron. Soc.* **498** (2020) 2492 [2007.08994].
- [30] EBOSS collaboration, *The Completed SDSS-IV extended Baryon Oscillation Spectroscopic Survey: BAO and RSD measurements from anisotropic clustering analysis of the Quasar Sample in configuration space between redshift 0.8 and 2.2*, *Mon. Not. Roy. Astron. Soc.* **500** (2020) 1201 [2007.08998].
- [31] EBOSS collaboration, *The completed SDSS-IV extended Baryon Oscillation Spectroscopic Survey: BAO and RSD measurements from the anisotropic power spectrum of the quasar sample between redshift 0.8 and 2.2*, *Mon. Not. Roy. Astron. Soc.* **499** (2020) 210 [2007.08999].
- [32] EBOSS collaboration, *The Completed SDSS-IV extended Baryon Oscillation Spectroscopic Survey: Growth rate of structure measurement from anisotropic clustering analysis in configuration space between redshift 0.6 and 1.1 for the Emission Line Galaxy sample*, *Mon. Not. Roy. Astron. Soc.* **499** (2020) 5527 [2007.09009].
- [33] EBOSS collaboration, *The Completed SDSS-IV extended Baryon Oscillation Spectroscopic Survey: measurement of the BAO and growth rate of structure of the emission line galaxy sample from the anisotropic power spectrum between redshift 0.6 and 1.1*, *Mon. Not. Roy. Astron. Soc.* **501** (2021) 5616 [2007.09008].
- [34] EBOSS collaboration, *The Completed SDSS-IV Extended Baryon Oscillation Spectroscopic Survey: Baryon Acoustic Oscillations with Ly α Forests*, *Astrophys. J.* **901** (2020) 153 [2007.08995].
- [35] A.G. Riess et al., *A Comprehensive Measurement of the Local Value of the Hubble Constant with 1 km s⁻¹ Mpc⁻¹ Uncertainty from the Hubble Space Telescope and the SH0ES Team*, *Astrophys. J. Lett.* **934** (2022) L7 [2112.04510].
- [36] L. Breuval, A.G. Riess, S. Casertano, W. Yuan, L.M. Macri, M. Romaniello et al., *Small Magellanic Cloud Cepheids Observed with the Hubble Space Telescope Provide a New Anchor for the SH0ES Distance Ladder*, **2404.08038**.
- [37] A. Notari, M. Redi and A. Tesi, *Consistent Theories for the DESI dark energy fit*, **2406.08459**.
- [38] F. Couchot, S. Henrot-Versillé, O. Perdureau, S. Plaszczyński, B. Rouillé d'Orfeuil, M. Spinelli et al., *Cosmological constraints on the neutrino mass including systematic uncertainties*, *Astron. Astrophys.* **606** (2017) A104 [1703.10829].
- [39] D. Wang, O. Mena, E. Di Valentino and S. Gariazzo, *Updating neutrino mass constraints with Background measurements*, **2405.03368**.
- [40] L. Amendola et al., *Cosmology and fundamental physics with the Euclid satellite*, *Living Rev. Rel.* **21** (2018) 2 [1606.00180].
- [41] R. Trotta, *Bayes in the sky: Bayesian inference and model selection in cosmology*, *Contemp. Phys.* **49** (2008) 71 [0803.4089].

Appendix

A Combined analysis with SH0ES

Let us explore the effect of combining with SH0ES on neutrino masses.

First, in the context of Λ CDM, we can see in Fig. 4 that, due to the degeneracy between H_0 and $\sum m_\nu$, a combination with SH0ES would cause a dramatically tighter constraint on $\sum m_\nu$. In this case, the would-be constraint from the combination **P20_H+DESI+Pantheon**

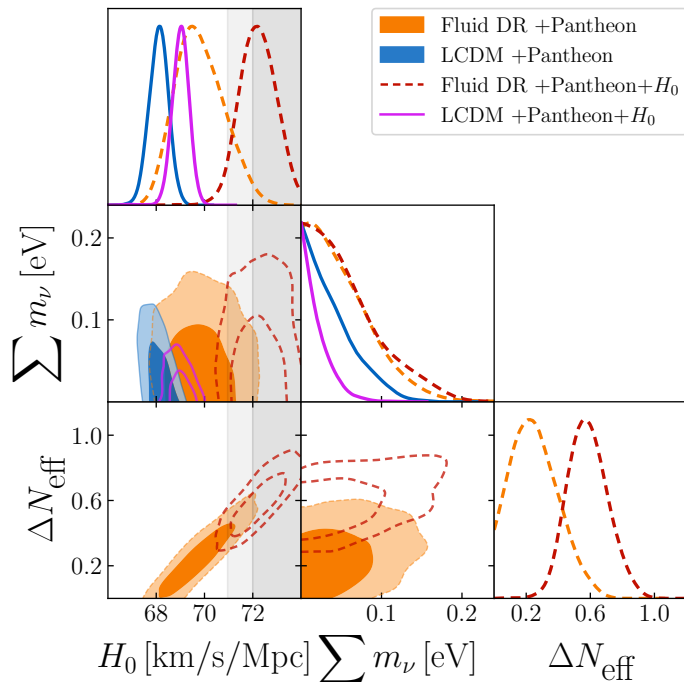


Figure 4: One- and two-dimensional posteriors for H_0 , $\sum m_\nu$, and ΔN_{eff} in both ΛCDM and the fluid DR model, fitting to **P20_H+DESI+Pantheon** and the same set with the addition of **H₀**. The inner and outer two-dimensional contours give the 1- and 2- σ confidence intervals, respectively. The dark and light gray bands show the 1- and 2- σ confidence intervals from the measurement of H_0 by the SH0ES collaboration.

+H₀ is $\sum m_\nu < 0.055$ eV, putting this constraint in conflict with neutrino oscillation experiments. Note that that the datasets in this combination are in great tension and therefore this combination is not justified.

Instead, in the case of fluid DR, the degeneracy between H_0 and $\sum m_\nu$ is no longer present. As seen in Table 3, this means that the constraint on $\sum m_\nu$ does not become tighter when adding SH0ES (now justified due to the lesser tension); in fact, it becomes even a bit weaker (shifting from < 0.13 eV with **P20_H+DESI+Pantheon** to < 0.15 eV when adding **+H₀**). Fig. 4 exhibits this as well, seen in the fact that the one-dimensional posterior for $\sum m_\nu$ is not made tighter by SH0ES.

B Neutrino mass posteriors fit to a Gaussian

We discuss now an assessment of whether the neutrino mass posteriors are peaked at would-be negative values of the neutrino mass, as was considered in [5, 6]. To do so, we can take the posteriors which are inferred when using a prior of $\sum m_\nu > 0$, as we have done in this work, and fit them to the tail of a Gaussian. Then, one can project where the preferred peak would lie if the fit were to extend to negative masses. Note that in [6], a different method is proposed.

We see in Fig. 3 that for some datasets, the $\Lambda\text{CDM} + \sum m_\nu$ model exhibits distributions that would peak at negative values. However, the inclusion of supernovae data drives these peaks closer to zero, mostly due to the DES-SN5YR supernovae. Also, when combining the

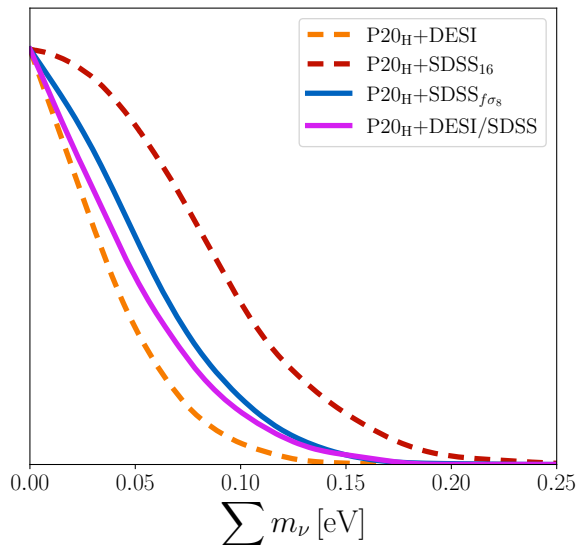


Figure 5: One-dimensional posteriors for $\sum m_\nu$, fitting to combinations of **P20_H** with different BAO datasets: **DESI**, **SDSS₁₆**, **SDSS_{f σ_8}** , or **DESI/SDSS**.

DESI BAO and SDSS BAO measurements along with DES-SN5YR supernovae, we can see even a peak at positive values. Further, using the same technique underscores the fact that in the Λ CDM+ $\sum m_\nu$ + Fluid DR model, the peaks are definitively driven to positive values of $\sum m_\nu$.

C Constraints from various BAO measurements

Fig. 5 gives the posteriors for $\sum m_\nu$ comparing the effects of different BAO datasets, as discussed in Section 3.3.